Back-Face Bragg Diffraction from a Perfect and Ultralightly Deformed Thick Crystal

M. Agamalian,[1] E. Iolin,[2] L. Rusevich,[2] C. J. Glinka,[3] and G. D. Wignall[1]
[1]*Oak Ridge National Laboratory, Oak Ridge, Tennessee 37831*
[2]*Institute of Physical Energetics, Riga, LV-1006, Latvia*
[3]*National Institute of Standards and Technology, Gaithersburg, Maryland 20899*
(Received 17 February 1998)

The intensity of neutrons Bragg diffracted from the back face of a 9 mm thick slab-shaped Si(111) analyzer crystal has been measured experimentally at the ORNL double crystal diffractometer and calculated theoretically. The back-face rocking curve of a strain-free perfect crystal contains two symmetrical peaks which become asymmetrical under an ultrasmall static deformation strain (bending with a radius of tens of km). The asymmetry is shown to be a sensitive measure of both the magnitude and direction of bending. [S0031-9007(98)06594-6]

PACS numbers: 62.20.–x, 61.12.Ex

The high transparency of silicon for thermal neutrons creates a unique opportunity to study total Bragg diffraction from a thick crystal (with the thickness $T \sim 1$ cm). Such experiments cannot be done with conventional x-ray radiation which cannot penetrate to the back face of a thick crystal. This property of neutron radiation was originally used by C. G. Shull in the early 1970s to measure separately the front-face (FF), back-face (BF), and end-face Bragg reflections from a thick Si crystal by scanning a narrow cadmium slit across the exiting beam [1,2]. However, all of these experiments were carried out in the conditions when the crystal under study was set up at a chosen angle of incidence, $\theta = \theta_B$, or slightly deviated from the exact Bragg angle, θ_B, and did not move while the detector was scanned across the diffracted beam.

The angular dependence of the intensity of BF reflection, $I_{BF}(\theta - \theta_B)$, on θ was measured for the first time at the ORNL Bonse-Hart double crystal diffractometer (DCD) [3]. In that experiment the short plate of the Si(111) analyzer channel-cut crystal 3 was covered by Cd, as shown in Fig. 1, to block the FF reflected beam and measure only the BF reflection from the long plate. The incident four-bounce neutron beam (wavelength $\lambda = 2.59$ Å, $\theta_B = 24.4°$) was formed by a sequence of reflections from the single-bounce premonochromator, followed by a triple-bounce channel-cut monochromator crystal (see Fig. 1). The intensity of the experimental BF rocking curve (BFRC), normalized by the peak intensity of the FF reflection, is shown in Fig. 2 (open circles) as a function of the dimensionless angular parameter of dynamical diffraction theory, $y = (\theta - \theta_B)/\delta\theta_B$, where $\delta\theta_B = b_c e^{-W}|F_S|N\lambda^2/\pi \sin\theta_B$ is the half-width of the Darwin plateau, b_c is the atomic coherent scattering length, e^{-W} is the Debye-Waller factor, F_S is the structure factor, and N is the number of unit cells per unit volume (in our case $\theta - \theta_B = 1$ arc sec corresponds to $y = 1.2$). The BFRC (Fig. 2) contains two sharp peaks at $y = \pm 2.2$ and a deep minimum at $y = 0$, in contrast to the FF rocking curve (FFRC) from a perfect crystal which has one peak at $y = 0$.

The BFRC can be derived from the classical dynamical diffraction theory using the condition (see, e.g., in [4]) that the intensity partially transmitted into a transparent crystal in the vicinity of the Bragg angle can be written as $1 - R_D(y)$, where $R_D(y)$ is the Darwin reflectivity function [5]

$$\begin{aligned} R_D(y) &= 1, \qquad |y| \le 1, \\ R_D(y) &= [|y| - (y^2 - 1)^{0.5}]^2, \qquad |y| > 1. \end{aligned} \tag{1}$$

Thus, inside the crystal $1 - R_D(y) = 0$, when $|y| \le 1$, and the intensity transmits into the crystal only when $y < -1$ or $y > +1$, which leads to the appearance of the two peaks in the BFRC, derived as the following convolution [6]:

$$\begin{aligned} I_{BF}(y)/I_{FF}(y = 0) &= \int [R_D^n(y_1)[1 - R_D(y + y_1)]^2 \\ &\quad \times R_D(y + y_1)\, dy_1, \end{aligned} \tag{2}$$

where $I_{BF}(y)$ and $I_{FF}(y = 0)$ are the intensities of the BF and FF reflected beams, respectively, $R_D^n(y_1)$ if the Darwin reflectivity function of the monochromator with n reflections, and $[1 - R_D(y)]^2 R_D(y)$ is the BF reflectivity function of the analyzer [7]. Profiles of the BFRCs, calculated from Eq. (2) for the single-bounce ($n = 1$) and four-bounce ($n = 4$) monochromators (Fig. 2, dotted and solid lines, respectively), show two sharp peaks, the resolution

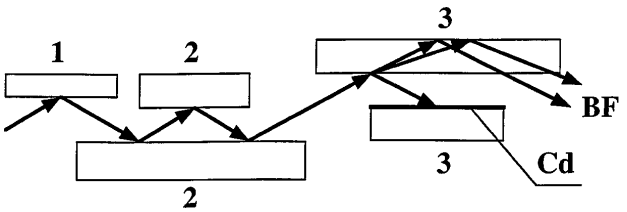

FIG. 1. BF reflection from the long plate of channel-cut crystal. 1: 2 mm thick perfect Si(111) crystal premonochromator; 2: triple-bounce channel-cut crystal monochromator; 3: triple-bounce channel-cut crystal analyzer with the short plate covered by Cd absorber.

 0031-9007/98/81(3)/602(4)$15.00

of which improves significantly when the number of reflections in the monochromator is increased. The theoretical BFRC (curve 2), corresponding to the optical scheme in Fig. 1, agrees well with the rather symmetrical experimental BFRC of the long plate of the channel-cut analyzer crystal.

However, Eq. (2), based on classical dynamical diffraction theory, does not describe the asymmetry recently observed at the ORNL DCD [6] for the BFRC of the 9 mm thick single-bounce Si slab-shaped crystal (see experimental data in Fig. 3). The setup for this and the following experiments can be imagined from Fig. 1 by simply taking out of consideration the short plate of the channel-cut crystal analyzer 3 and consider the long plate as a single-bounce crystal. That measurement differed from the observation of the BFRC of the channel-cut crystal described above in that the slab-shaped crystal was affixed to the plastic supporting plate by epoxy resin, which could be a source of deformation strains. Thus, calculations taking into consideration the influence of external force fields on the neutron diffraction from a perfect crystal (see, e.g., in [8–10]) have been carried out assuming the presence of ultraweak static deformation strains in the crystal under study. The model is based on the dynamical two-wave diffraction theory of deformed crystals in the Bragg case (see, e.g., [11]), according to which the neutron wave field inside the crystal can be analyzed by the system of Takagi-Taupin equations:

$$\begin{aligned} -i(\partial\Psi_0/\partial X) - i(\partial\Psi_0/\partial Z)\tan\theta_B + (\Delta k_0/2)\exp(-i\mathbf{H}\cdot\mathbf{l}_c)\Psi_h = 0, \\ -i(\partial\Psi_h/\partial X) - i(\partial\Psi_h/\partial Z)\tan\theta_B + (\Delta k_0/2)\exp(+i\mathbf{H}\cdot\mathbf{l}_c)\Psi_0 = 0, \end{aligned} \tag{3}$$

where Ψ_0 and Ψ_h are the amplitude of the incident and diffracted beams, respectively, θ_B is the Bragg angle, X and Z are the Cartesian coordinates directed parallel and perpendicular to the FF of the crystal, respectively (Fig. 4), $\mathbf{H}$ is the scattering vector, $\mathbf{l}_c$ is the displacement vector of a nucleus from its position in a perfect crystallographic lattice due deformation strains, $\Delta k_0 = 2\pi/l_p$ is the gap between two branches of the neutron dispersion surface of the crystal, $k_0 = 2\pi/\lambda$ is the wave vector of the primary beam, λ is the wavelength, and l_p is the extinction length. The gap, Δk_0, is connected with the half-width of the Darwin table, Eq. (1), by the formula $\delta\theta_B = \Delta k_0/2k_0\sin\theta_B$. The smooth static inhomogeneous deformation strain leads to an adiabatic motion of tie points along the dispersion surface [11], which can be modeled as

$$\mathbf{H}\cdot\mathbf{l}_c = 2AS_0^2 + 4BS_0S_d + 2CS_d^2, \tag{4a}$$

$$X = (S_0 + S_d)\cos\theta_B, \qquad Z = (S_0 - S_d)\sin\theta_B, \tag{4b}$$

where S_0 and S_d are the coordinates directed along the incident and diffracted beam, respectively (Fig. 4), and A, B, and C are the numerical parameters. After the following coordinate transformations in Eqs. (4a) and (4b): $X \to Xl_p/\pi, Z \to Z\tan\theta_B/\pi$, $A \to a(\pi\cos\theta_B/l_p)^2$, $B \to b(\pi\cos\theta_B/l_p)^2$, $C \to c(\pi\cos\theta_B/l_p)^2$, where a, b, and c are the parameters which characterize the deformation, the product $\mathbf{H}\cdot\mathbf{l}_c$ in the dimensionless form is

$$\mathbf{H}\cdot\mathbf{l}_c = a/2(X+Z)^2 + b(X^2 - Z^2) + c/2(X-Z)^2. \tag{5}$$

And after the substitutions, $\Psi_0 \to \Psi_0\exp(-ic/2(X - Z)^2 - ib/2(X^2 - Z^2) + ibXZ)$, $\Psi_h \to \Psi_h\exp(+ia/2(X+Z)^2 + ib/2(X^2 - Z^2) + ibXZ)$, system (3) can be rewritten as

$$\begin{aligned} i(\partial\Psi_0/\partial X) + i(\partial\Psi_0/\partial Z) - 2bZ\Psi_0 - \Psi_h = 0, \\ -i(\partial\Psi_h/\partial X) + i(\partial\Psi_h/\partial Z) + 2bZ\Psi_h + \Psi_0 = 0. \end{aligned} \tag{6}$$

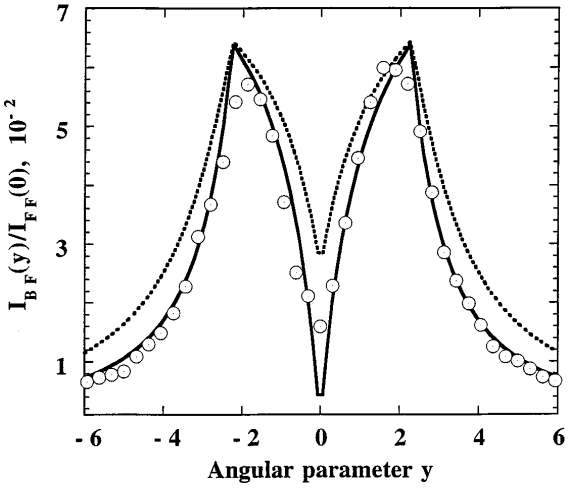

FIG. 2. BFRCs, measured experimentally from the long plate of channel-cut crystal analyzer (open circles), and calculated by Eq. (2) for $n = 1$ (dotted line) and for $n = 4$ (solid line).

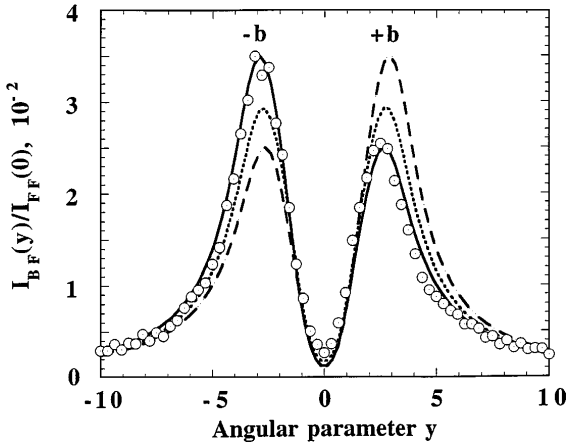

FIG. 3. Experimental BFRCs of the initially deformed 9 mm Si(111) crystal (open circles) and results of calculations for $b = -1.43 \times 10^{-4}$ (solid line), $b = 0.0$ (dotted line), and $b = +1.43 \times 10^{-4}$ (dashed line).

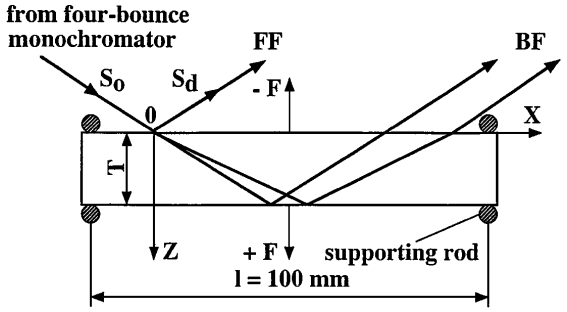

FIG. 4. Geometry of BFRC measurements with deformation control.

The quasi-impulse of neutron wave, Q, along the crystal surface (coordinate X) is now conserved and after the substitution, $\Psi_{0,h} \rightarrow \Psi_{0,\mathrm{h}} \exp(iQX)$, Eq. (6) can be simplified [12]:

$$\begin{aligned} i(\partial\Psi_0/\partial Z) - (Q + 2bZ)\Psi_0 - \Psi_h = 0\,, \\ -i(\partial\Psi_h/\partial Z) + (Q + 2bZ)\Psi_h + \Psi_0 = 0\,. \end{aligned} \tag{7}$$

Solution of system (7) with the boundary conditions, $\Psi_0(Q, Z = 0) = 1, \Psi_h(Q, Z = T) = 0$, where T is the crystal thickness (Fig. 4), allows one to obtain the amplitude of the diffracted beam, $\Psi_{\mathrm{h}}(Q, Z = 0)$ and the final expression for the intensity of BFRC of the deformed crystal is given by

$$I_{\mathrm{BF}}(y) \sim \iiint R_{\mathrm{D}}^4(Q - y)A(Q_d)G(Q - Q_d)A^* \times (Q_d')G(Q - Q_d')\,dQ_d\,dQ_d'\,dQ\,, \tag{8}$$

where $R_{\mathrm{D}}^4(Q - y)$ in the Darwin reflectivity function of the four-bounce monochromator (Fig. 1), $A(Q_d) = \int\int \Psi_h(Q, Z = 0) \exp[i(Q - Q_d)Z + i(b + c)/2X^2]\,dX\,dQ$, is the integrated amplitude of the BF diffracted beam, $G(Q) = \int G(Q) \exp(-iQX)\,dX$ is the transmission function of the detector slit and Q, Q_d are the variables of integration. Thus, the intensity of BFRC, $I_{\mathrm{BF}}(y)$, does not depend on the parameter a [see Eq. (5)] and is controlled by the two independent parameters, b and c, which simulate the deformation strain. Computer analysis of Eq. (8) has shown that variation of c leads mostly to displacements of the whole BFRC with respect to $y = 0$ without significant changes of the profile. Absence of this displacement in the experimental BFRCs collected in the present study corresponds to the condition when $c + b = 0$, thus the expression for the integrated amplitude $A(Q_d)$ in Eq. (8) can be simplified, $A(Q_d) = 2\pi\Psi_h(Q_d, Z = 0)$, where $\Psi_h(Q_d, Z = 0)$ depends only on the parameter b. This parameter controls the asymmetry of the BFRC as it is shown in Fig. 3: the curve is symmetrical (dotted line) when $b = 0$ and becomes asymmetrical (solid and dashed lines) when $|b| > 0$. The sign and value of b is related to the direction and value of the deformation force, **F**, respectively (see Fig. 4).

Insight into the physics of the BF reflection from a deformed transparent thick crystal may be obtained via the quasiclassical approximation [13,14]. It is known that influence of the inhomogeneous deformation strain on the Bragg diffracted intensity is different for the tie points located at the right, $y \approx 1$, and left, $y \approx -1$, sides of the Darwin plateau [12]. Therefore, the relative perturbation of the BF diffracted intensity as a result of deformation strain has been calculated for the right (+) and left (−) branches of the dispersion surface:

$$\delta I_h^{\pm}/I_h^{\pm} = 4bT(y^2 - 1)^{-0.5}, \tag{9}$$

where $I_h^{\pm}$ is the intensity BF diffracted from an undeformed crystal and $\delta I_h^{\pm}$ is the deviation of $I_h^{\pm}$ with the deformation strain. Equation (9) explicitly shows the dependence of $\delta I_h^{\pm}/I_h^{\pm}$ on the parameter b and explains an extremely high sensitivity of the BFRC to inhomogeneous deformation strains in the vicinity of $y \approx \pm 1$. It is useful to note that $\delta I_h^{\pm}/I_h^{\pm}$ is proportional to the crystal thickness T; thus the effect of BFRC asymmetry should be stronger the thicker the crystal is.

The theoretical BFRC calculated by Eq. (8) for $b = -1.43 \times 10^{-4}$ (solid line in Fig. 3) is in good agreement with the experimental result which supports the hypothesis that in this particular case the initial static deformation strain in the crystal was produced by stress, introduced by the crystal holder. The radius of crystal bending, $R \cong 28$ km, and displacement of the central point of the crystal, $dZ \cong 0.045\ \mu$m, have been estimated from the fitting curve (Fig. 3, solid line) by the equations

$$R \cong (H/2b)\,(l_p/\pi)^2, \tag{10a}$$

$$dZ = R - (R^2 - l^2/4)^{0.5}, \tag{10b}$$

where $l = 100$ mm is the length of the crystal along the X coordinate (Fig. 4). The deformation strain in a perfect crystal can also be calculated from a slope of experimental diffraction curves (Laue case) in the region of Pendellösung fringes [15]. Similar values of the ultrasmall deformation strains (with the bending radii $8.5 \leq R \leq 23$ km) of the thick Si crystals ($2.3 \leq T \leq 9.8$ mm), obtained in the Laue geometry was reported by Shull [1].

The results of theoretical calculations (Fig. 3) have been verified by the additional measurements of BFRCs of the same 9 mm thick crystal with the controlled ultrasmall deformation strains. In this experiment the crystal position has been fixed by four side supporting rods and the sequential deformation force in the range $-150 \leq F \leq +150$ g (1 g = 980.665 dynes) with the step $|\Delta F| = 50$ g has been applied perpendicularly to the diffractive surfaces in both directions (see Fig. 4). The BFRC, measured for $F = -150$ g, $F = 0.0$ g, and $F = +150$ g, is shown in Fig. 5 together with the corresponding theoretical rocking curves, calculated by Eq. (8). This diagram demonstrates a dramatic difference in profiles of the BFRCs of the deformed and strain-free crystal, while these ultrasmall values of deformation strain

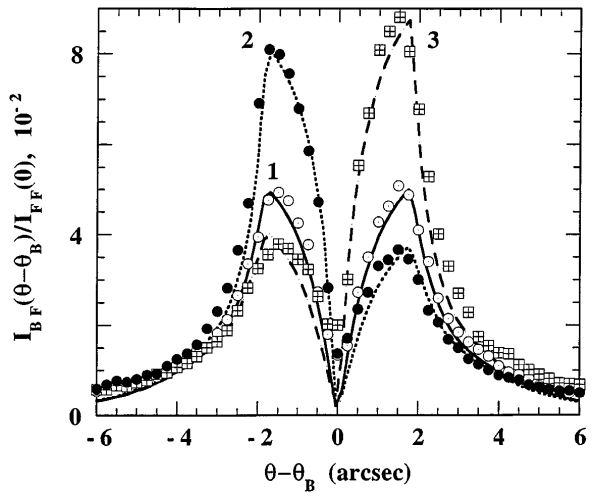

FIG. 5. Experimental and theoretical BFRCs. 1: F = 0.0 g, 2: F = −150 g, and 3: F = +150 g.

have been found undetectable in the measurements of the corresponding FFRCs.

The asymmetry of BFRCs of the deformed crystal can be defined by the standard parameter:

$$A(F) = [I_m(F)^+ - I_m(F)^-]/[I_m(F)^+ + I_m(F)^-], \tag{11}$$

where $I_m(F)^+$ and $I_m(F)^-$ are the peak intensities of the right and left maxima of the BFRC, respectively. Figure 6 shows that the theoretical function $A(F)$ is almost linear (solid line) in the chosen range of deformation forces, $-150 \le F \le +150$ g, which is in good agreement with the experimentally obtained values (opened circles) of this parameter. Therefore, it is possible to determine from Fig. 6 that $A(F) = 0.25$, calculated for the experimental BFRC in Fig. 3 (open circles), corresponds to the deformation force $F = -50$ g. If it is so, one can verify the values, $R \cong 28$ kg and $dZ = 0.045$ μm, by the direct macroscopic experiment, when the crystal under study has been loaded by $F = 10.5$ kg and displacement of the central point ($dZ = 7.6$–10 μm) has been measured by the indicator with the accuracy ± 0.25 μm. This result, linearly extrapolated to $F = 50$ g, assuming that the deformation strain is completely elastic, gives the value of $dZ = 0.036$–0.048 μm, which agrees with that calculated from the neutron experiment by Eqs. (10a) and (10b).

The newly observed unusual profile of the BFRC can be interpreted by the classical dynamical diffraction theory, which, however, does not explain the asymmetry of the BFRC. This effect has been modeled theoretically in terms of the dynamical two-wave scattering from deformed crystals and verified by the neutron diffraction experiment with the controlled ultrasmall static bending of the crystal. The results of this study show the extremely high sensitivity of the BFRC to ultrasmall deformation strains, which gives the opportunity to utilize this effect for the analysis of local residual stresses in single crystals.

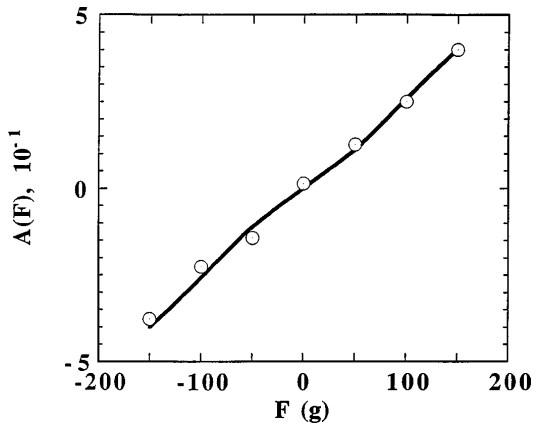

FIG. 6. Parameter $A(F)$ calculated theoretically (solid line) and obtained from experimental BFRCs (open circles).

The authors thank S. A. Werner (University of Missouri), M. Hart (Brookhaven National Laboratory), T. M. Sabine (Australian Nuclear Science and Technology Organization), and J. B. Roberto and H. A. Mook (ORNL) for fruitful discussions. The research at Oak Ridge was supported by the Division of Material Science, U.S. Department of Energy under Contract No. DE-AC5-96OR22464 with Lockheed Martin Energy Research Corporation and in part supported by the Oak Ridge National Laboratory Postdoctoral Research Associates Program administered jointly by the Oak Ridge National Laboratory and the Oak Ridge Institute for Science and Education. Some of this work is based upon activities supported by the National Science Foundation under Agreement No. DMR-9423101. Commercial product names have been used in this report to describe fully the experimental methods and do not constitute or imply endorsement by the National Institute of Standards and Technology for any purpose.

[1] C. G. Shull, Appl. Crystallogr. **6**, 257 (1973).
[2] A. Zeilinger, C. G. Shull, J. Artur, and M. A. Horne, Phys. Rev. A **28**, 487 (1983).
[3] M. Agamalian, R. Triolo, and G. D. Wignall, J. Appl. Crystallogr. **30**, 345 (1997).
[4] U. Bonse and M. Hart, Z. Phys. **194**, 1 (1966).
[5] C. G. Darwin, Philos. Mag. **27**, 675 (1914).
[6] M. Agamalian *et al.*, J. Appl. Crystallogr. **31**, 235 (1998).
[7] T. Takahashi and M. Hashimoto, Phys. Lett. A **200**, 73 (1995).
[8] S. A. Werner, Phys. Rev. B **21**, 1774 (1980).
[9] S. Takagi, Acta Crystallogr. **15**, 1311 (1962).
[10] D. Taupin, Bull. Soc. Fr. Mineral. Cristallogr. **84**, 51 (1961).
[11] Z. G. Pinsker, *Dynamical Scattering of X-Rays in Crystals* (Springer-Verlag, Berlin, 1978).
[12] E. M. Iolin, A. V. Muromtsev, and L. L. Rusevich, Phys. Status Solidi (b) **184**, 69 (1994).
[13] N. Kato and Y. Ando, J. Phys. Soc. Jpn. **21**, 964 (1966).
[14] K. Kambe, Z. Naturforsch. **20A**, 770 (1965).
[15] M. Hart, Z. Phys. **198**, 269 (1966).